

## Carrier dynamics in laterally strain-modulated InGaAs quantum wells

Vadim Talalaev, Jens W. Tomm,<sup>a)</sup> and Thomas Elsaesser

*Max-Born-Institut für Nichtlineare Optik und Kurzzeitspektroskopie, Max-Born-Strasse 2 A, 12489 Berlin, Germany*

Ute Zeimer, Jörg Fricke, Arne Knauer, Heiko Kissel,<sup>b)</sup> and Markus Weyers

*Ferdinand-Braun-Institut für Höchstfrequenztechnik, Gustav-Kirchhoff-Strasse 4, 12489 Berlin, Germany*

Georgiy G. Tarasov

*Institute of Semiconductor Physics, National Academy of Sciences, Prospect Nauki 45, 03028 Kiev, Ukraine*

J. Grenzer and U. Pietsch

*Institut für Physik, Universität Potsdam, Am Neuen Palais 10, 14469 Potsdam, Germany*

(Received 29 April 2005; accepted 31 October 2005; published online 19 December 2005)

We investigate the transient recombination and transfer properties of nonequilibrium carriers in an  $\text{In}_{0.16}\text{Ga}_{0.84}\text{As}/\text{GaAs}$  quantum well (QW) with an additional lateral confinement implemented by a patterned stressor layer. The structure thus contains QW- and quantum-wire-like areas. At low excitation densities, photoluminescence (PL) transients from both areas are well described by a rate equation model for a three-level system with a saturable interlevel carrier transfer representing the lateral drift of carriers from the QW regions into the wires. Small-signal carrier lifetimes for QW, wires, and transfer time from QW to wire are 180, 190, and 28 ps, respectively. For high excitation densities the time constants of the observed transients increase, in agreement with the model. In addition, QW and wire PL lines merge indicating a smoothing of the potential difference, i.e., the effective carrier confinement caused by the stressor structure becomes weaker with increasing excitation. © 2005 American Institute of Physics. [DOI: 10.1063/1.2151248]

One of the key parameters employed in semiconductor quantum engineering is built-in strain, which is created during epitaxial growth. Subsequent strain modulation, e.g., by lateral patterning offers an additional degree of freedom for changing electronic potentials. Lateral confinement in a quantum well (QW) plane has been introduced by stressor structures and characterized by standard means.<sup>1,2</sup> In more recent studies, based on near-field scanning microscopy with a subwavelength spatial resolution, the original QW and the wirelike potential wells created within the QW by a stressor structure have been distinguished via their different photoluminescence (PL) spectra.<sup>3</sup> For the practical application of such structures, e.g., as the active region of devices such as diode lasers, however, knowledge about the behavior at very high carrier densities as well as about the transients of the nonequilibrium carriers within such complex systems is of utmost interest.

In this letter we address these two topics by time-resolved PL measurements carried out on extensively pre-characterized samples with a QW wire structure induced in an InGaAs QW by a patterned strained GaInP layer. PL transients representing the transient population of QW and wires turn out to be well described within a rate equation model for a three-level system with saturable interlevel carrier transfer, which is in our particular structure the lateral drift<sup>4</sup> of carries from the QW regions into the wires. Small-signal carrier lifetimes for QW, wires, and transfer time from QW to wire are  $(180 \pm 10)$ ,  $(190 \pm 10)$ , and  $(28 \pm 5)$  ps, respectively. For high excitation densities the time constants of the observed

transients increase. Our rate-equation model explains this effect as well. In addition, QW and wire PL lines merge at high carrier densities, indicating a smoothing of the potential difference between both.

Samples were grown at  $T=550$  °C by metalorganic vapor phase epitaxy on GaAs (100) substrates using the standard precursors trimethylindium, trimethylgallium, arsine, and phosphine. The layer sequence consists of a 10-nm-thick  $\text{In}_{0.16}\text{Ga}_{0.84}\text{As}$  QW ( $\epsilon=-1.14\%$ ), embedded between a 100-nm-thick GaAs buffer and a 10-nm GaAs etch stop layer, followed by a 40-nm-thick  $\text{In}_{0.387}\text{Ga}_{0.613}\text{P}$  stressor layer with a pseudomorphic tensile strain of 0.73%. A 12-nm-thick GaAs cap layer finishes the vertical layer sequence. The lateral grating was prepared by holographic photolithography and subsequent wet chemical etching down through the  $\text{In}_{0.387}\text{Ga}_{0.613}\text{P}$  to the GaAs etch stop layer, resulting in a trapezoidal grating with a period of 500 nm and {111} sidewalls. The trenches and ridges run parallel to the [1-10] direction. The valley width is 90 nm [Fig. 1(a)]. Unpatterned QW areas serve as reference. The removal of the stressor layer during the creation of the trenches reduces the compression of the QW at these positions, i.e., adds tensile strain into the QW underneath the trenches. Since tensile strain causes band-gap shrinkage, quasi-one-dimensional potential wells are formed under the trenches. Therefore, we call these tensed QW regions “wires,” whereas the 410-nm QW region between these wires is further called the QW. The shape of the confinement potential for this particular device architecture is modeled within the framework of elasticity theory,<sup>5</sup> and shown in Fig. 1(b) versus the same lateral scale as Fig. 1(a). The inset in Fig. 1(b) depicts a level scheme, illustrating recombination processes from the QW and wire regions as well as carrier drift from the QW to the wires, not includ-

<sup>a)</sup> Author to whom correspondence should be addressed; electronic mail: tomm@mbi-berlin.de

<sup>b)</sup> Present address: DILAS Diodenlaser GmbH, Galileo-Galilei-Strasse 10, 55129 Mainz, Germany.

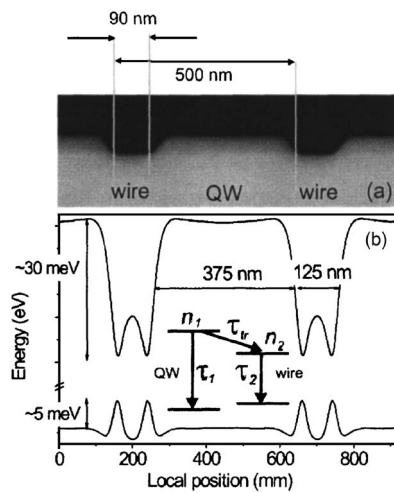


FIG. 1. Characterization of the QW wire sample. (a) Scanning electron microscope image at a cleaved cross section. (b) Potential of the QW wire structure as modeled by the finite element method within the framework of elasticity theory. The inset shows a level scheme illustrating recombination processes from the QW (index 1) and wire regions (index 2) as well as the carrier transfer from the QWs to the wires (index  $tr$ ), without taking into account the details of the semiconductor band structure.

ing the semiconductor QW bandstructure details.

Transient PL is excited by a mode-locked Ti:sapphire laser (Spectra Physics Tsunami) generating 80-fs pulses with a repetition rate of 81 MHz and a center wavelength of 775 nm. The laser beam is directed to the top of the structured epilayer, thus exciting both QW and wire areas. The PL from the sample is detected in reflection by a Hamamatsu synchroscan streak camera with an S1 cathode. From the geometry we expect a ratio of the PL signals of 375 nm:125 nm = 3:1; i.e., determined by the potential shape created by stressor-stripe width ratio [Fig. 1(b)]. The excitation flux per pulse is varied in the range of  $3 \times 10^9$ – $3 \times 10^{11}$  photons/cm<sup>2</sup>. The sample temperature is 10 K.

In Fig. 2, results of our spectrally and temporally resolved measurements are summarized. Figures 2(a) and 2(b) show streak-camera traces measured at an excitation flux of  $10^{10}$  photons/cm<sup>2</sup> per pulse. For all data sets time zero ( $t=0$ ) is set to the maximum of the excitation pulse ( $1/e$  decay time < 18 ps) as imaged by the detection system. For the PL from the unpatterned reference QW [Fig. 2(a)], we find an almost exponential PL decay described by a time constant of  $\tau_1 \sim 180$  ps and a delay between excitation and PL maxima of  $\sim 30$  ps. The value of  $\tau_1$  rises to  $\sim 230$  ps and the delay increases to  $\sim 70$  ps, when the pump flux is increased up to  $3 \times 10^{11}$  photons/cm<sup>2</sup>. Figure 2(b) displays comparable data from the QW-wire sample shown in Fig. 1. Obviously, the QW PL line remains spectrally unshifted but a second, red-shifted line appears 34 meV below the QW emission. Theoretical calculations for this particular structure predict a confinement potential of  $\sim 30$  meV for electrons and  $\sim 5$  meV for holes, whereas the steady-state PL characterization provides a line separation of 32 meV. Thus, we assign the low-energy emission in Fig. 2(b) to PL from the wire region of the sample. Figure 2(c) shows PL spectra as a function of the excitation, i.e., horizontal cross sections through images such as Fig. 2(b). Figure 3 shows PL transients from the QW wire sample for fixed photon energies of the emission, i.e., vertical cross sections through images such as Fig. 2(b). The de-

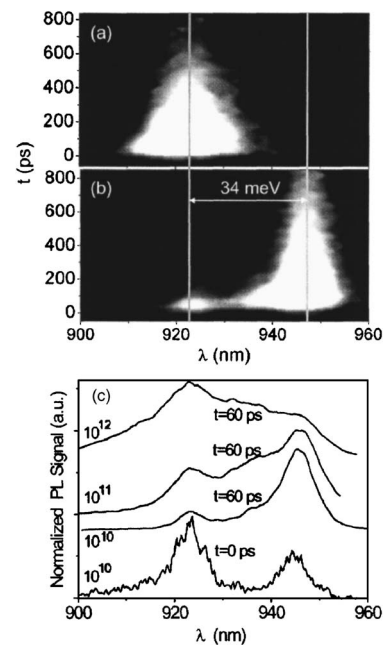


FIG. 2. Streak-camera images of the PL data from the unpatterned reference QW (a) and from the QW-wire sample (b) for an excitation flux per pulse of  $10^{10}$  photons/cm<sup>2</sup>. (c) PL spectra for increasing excitation flux per pulse (photons/cm<sup>2</sup>) taken at  $t=60$  ps, i.e., after most of the lateral transport took place. The reference spectrum at  $t=0$  (bottom) is representative for the initial population. In all cases  $t=0$  is set to the maximum of the excitation pulse as imaged by the detection system.

cay time of QW PL changes strongly with excitation density, and is characterized by  $\tau_1$  values of 28 and 240 ps for excitation fluxes of  $3 \times 10^9$  and  $3 \times 10^{11}$  photons/cm<sup>2</sup>, respectively. For the same range of excitation flux, the time constant of the wire PL decay  $\tau_2$  [see inset in Fig. 1(b)], increases from 190 to 500 ps. The wire PL becomes substantially weaker compared to QW PL and both lines merge into one broad band (see Fig. 2 on top).

In our experiments, the sample is excited well above the band edges of both QW and wire, i.e., electron-hole pairs are generated in the GaAs barriers from which they are transferred into the QW and wire. This process is reflected in the  $\sim 30$ -ps delay between the maximum of the excitation pulse at  $t=0$  and the temporal PL maxima of QW and wires. The delay measured here agrees well with the results of recent QW carrier capture time measurements by Hader *et al.*<sup>6</sup> The indirect population mechanism of QW and wire could be also responsible for the deviation between the expected initial QW/wire population ratio  $n_1(0)/n_2(0)=3$  and the experimental value of  $n_1(0)/n_2(0)=2.5$ ; see spectrum taken at  $t=0$  at the bottom of Fig 2(c). A superproportional drift of carriers from the barrier towards the wire compared to the QW is a likely microscopic explanation.

A quantitative analysis of carrier transfer and recombination requires modeling of the carrier distributions in QW and wire. The complex lateral confinement potential and the uncertainty of the relevant local parameters make calculations of the detailed electronic bandstructure and carrier distributions difficult, and require a very high numerical effort. We thus use a highly simplified three-level rate equation model to approximate carrier dynamics by exponential kinetics of the total carrier populations of QW and wire. A key ingredient is the interlevel carrier transfer, which we assume to be saturable and to account for Pauli blocking of wire

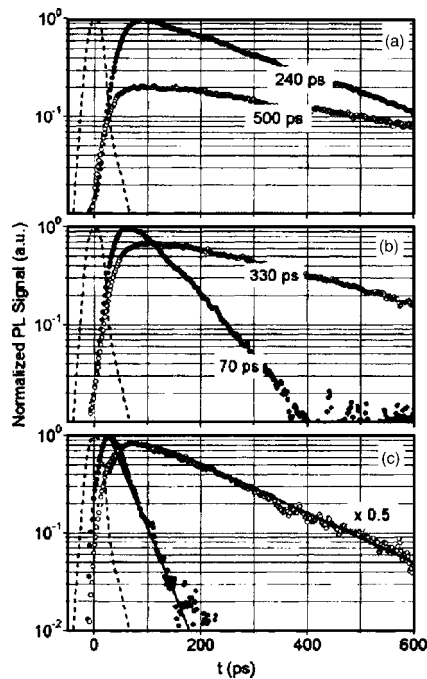


FIG. 3. PL transients from the QW wire sample. Full circles represent PL data from the QW, whereas open circles indicate data that stem from the wire PL. The excitation pulse, as imaged by the complete detection system (apparatus function) is given as a dashed line. The excitation flux per pulse in (a), (b), and (c) is  $3 \times 10^{11}$ ,  $3 \times 10^{10}$ , and  $3 \times 10^9$  photons  $\times$  cm $^{-2}$ , respectively. The full lines in (c) represent a normalized fit according Eqs. (1) with initial populations of  $n_1(0)=0.25$  and  $n_2(0)=0.1$  as well as time constants  $\tau_1=180$ ,  $\tau_2=190$ ,  $\tau_{tr}=28$ , and a delay time of 27 ps. The numbers given in the figure represent the time constants ( $1/e$  decay) as determined from the slopes of the respective data.

states by the carrier population. The populations of the QW,  $n_1(t)$ , and the wire,  $n_2(t)$ , are given by the equation system,

$$\begin{aligned} \frac{dn_1(t)}{dt} &= -\frac{n_1(t)}{\tau_1} - \frac{n_1(t)[1-n_2(t)]}{\tau_{tr}}, \\ \frac{dn_2(t)}{dt} &= -\frac{n_2(t)}{\tau_2} + \frac{n_1(t)[1-n_2(t)]}{\tau_{tr}}, \end{aligned} \quad (1)$$

where  $\tau_1$  and  $\tau_2$  are the recombination times of QW and quantum wire, respectively and  $\tau_{tr}$  is a time constant accounting for the lateral real-space transfer. The excitation flux per pulse of  $3 \times 10^9$  photons/cm $^2$ , the ratio  $n_1(0)/n_2(0)=2.5$ , and  $\tau_1=180$  ps are the parameters, which are fixed by the experiment. In addition, we introduce the initial delay of  $\sim 30$  ps that has been addressed before. From the fit of the data in Fig. 3(c), we extract values of  $\tau_2=(190 \pm 10)$  and  $\tau_{tr}=(28 \pm 5)$  ps, where the uncertainties are estimated by systematic variation of the fitting parameters. The full lines are calculated by a numerical solution of Eqs. (1), assuming initial population of  $n_1(0)=0.25$  and  $n_2(0)=0.1$  as well as time constants  $\tau_1=180$ ,  $\tau_2=190$ , and  $\tau_{tr}=28$  ps. This small value for  $\tau_{tr}$  is confirmed by the inverted intensity ratio of wire- and QW-PL intensity when varying  $t$  from  $t=0$  to  $t=60$  ps; see Fig. 2(c) bottom. Carrier transfer from the QW into the wire is due to drift-diffusion processes, where both the concentration gradient and the electric field originating from the lateral variation of the confinement potential act as driving forces. It should be noted that similar drift-diffusion times have been found in other QW/wire structures.<sup>7</sup> A very efficient carrier drift from the QW areas

to the wires is indicated. Despite the large difference in confinement potentials, e.g., for electrons  $V_{QW} \sim 150$  meV against the GaAs barriers and for the wire  $V_{wire} \sim 30$  meV against the QW,  $\tau_{tr}$  is comparable to the capture time of carriers from the GaAs barriers into the QWs.

For higher excitation densities of  $3 \times 10^{10}$  photons/cm $^2$  [Fig. 3(b)], the quality of the fits based on our simple model becomes poorer, mainly due to the filling of ground states and subsequent population of excited states within the QW. Nevertheless, if one takes into account the tenfold increased excitation by  $n_1(0)=2.5$  and  $n_2(0)=1$  and leaves all other parameters unchanged the model provides  $\sim 80$  and 250 ps for the  $n_1(t)$  and  $n_2(t)$  decays, respectively.<sup>8</sup> These values are to be compared with the experimental ones of 70 and 330 ps [Fig. 3(b)]. Thus, the tendency of increasing decay times is still qualitatively well described. Microscopically, state filling occurs and leads again to emission from all spatial regions as at  $t=0$ . This results in an enhancement of the high-energy wing of the QW PL spectra; see Fig. 2(c), from the bottom to the top. This reshaping of the emission spectrum is not accounted for in our simple model, and, thus, a more detailed model considering the intraband carrier distributions is required for an appropriate modeling of the decay time changes. Such a model needs to include the details of the band structure as well as the consideration of the spectral dependence of the transients as we have done earlier for the lateral carrier transfer between differently sized quantum dots.<sup>9</sup>

In conclusion, we have studied the recombination and transfer properties of nonequilibrium carriers in a QW with additional lateral confinement implemented by a stressor structure. Photoluminescence PL transients from the QW and wirelike potential wells demonstrate that carriers are exchanged between QW and wire through lateral drift processes. This behavior is modeled with the help of a simple three-level system with saturable interlevel carrier transfer. Small-signal carrier lifetimes for QW, wires and transfer time from QW to wire are determined to 180, 190 and 28 ps, respectively. For high excitation densities the time constants of the observed transients increase and QW and wire PL lines merge indicating a smoothening of the potential difference between both. Thus the effective carrier confinement caused by the stressor structure is found to become weaker with increasing carrier density.

<sup>1</sup>K. Kash, R. Bhat, D. D. Mahoney, P. S. D. Lin, A. Scherer, J. M. Worlock, B. P. Van der Gaag, M. Koza, and P. Grabbe, Appl. Phys. Lett. **55**, 681 (1989).

<sup>2</sup>Z. Xu, M. Wassermeier, Y. J. Li, and P. M. Petroff, Appl. Phys. Lett. **60**, 586 (1992).

<sup>3</sup>Zeimer, F. Bugge, S. Gramlich, V. Smirnitcki, M. Weyers, G. Tränkle, J. Grenzer, U. Pietsch, G. Cassabojs, V. Emiliani, and Ch. Lienau, Appl. Phys. Lett. **79**, 1611 (2001).

<sup>4</sup>We use the term "drift" in this context to describe the field enhanced diffusion of nonequilibrium carriers.

<sup>5</sup>J. Grenzer, U. Zeimer, S. A. Grigorian, S. Feranchuk, U. Pietsch, J. Fricke, H. Kissel, A. Knauer, and M. Weyers, Phys. Rev. B **69**, 125316 (2004).

<sup>6</sup>J. Hader, J. V. Moloney, and S. W. Koch, Appl. Phys. Lett. **85**, 369 (2004).

<sup>7</sup>A. Richter, M. Süptitz, D. Heinrich, Ch. Lienau, T. Elsaesser, M. Ramsteiner, R. Nötzel, and K. H. Ploog, Appl. Phys. Lett. **73**, 2176 (1998).

<sup>8</sup>The calculated transients at high densities are of course not strictly exponential. Therefore values for the  $1/e$  decays are estimates only.

<sup>9</sup>Yu. I. Mazur, J. W. Tamm, V. Petrov, G. G. Tarasov, H. Kissel, C. Walther, Z. Ya. Zhuchenko, and W. T. Masselink, Appl. Phys. Lett. **78**, 3214 (2001).